Neuroinformatics and Analysis of Connectomic Alterations Due to Cerebral Microhemorrhages in Geriatric Mild Neurotrauma

Alexander S. Maher
USC Davis School of Gerontology
University of Southern California
Los Angeles, CA, 90089, USA
amaher@usc.edu

Kenneth A. Rostowsky
USC Davis School of Gerontology
University of Southern California
Los Angeles, CA, 90089, USA
rostowsk@usc.edu

Nahian F. Chowdhury
USC Davis School of Gerontology
University of Southern California
Los Angeles, CA, 90089, USA
nfchowdh@usc.edu

Andrei Irimia
USC Davis School of Gerontology
University of Southern California
Los Angeles, CA, 90089, USA
irimia@usc.edu

ABSTRACT

Connectomics alterations associated with subtle forms of cerebrovascular neuropathology—such as cerebral microbleeds (CMBs)—can result in substantial neurological and/or cognitive deficits in victims of traumatic brain injury (TBI). Quantifying CMB-related connectome changes in mild TBI (mTBI) patients requires ingenious neuroinformatics to integrate structural magnetic resonance imaging (sMRI) with diffusion-weighted imaging (DWI) for patient-tailored profiling while preserving the data scientist's ability to implement population studies. Such solutions, however, can assist the refinement of rehabilitation protocols and streamline large-scale analysis while accommodating the heterogeneity of mTBI. This study describes a pipeline for the multimodal integration of sMRI/DWI/DTI to quantify white matter (WM) neural network circuitry alterations associated with mTBI-related CMBs. The approach incorporates WM streamline matching, topology-compliant streamline prototyping and along-tract analysis within a unified framework. When applied to the analysis of neuroimaging data acquired from both mTBI and healthy control volunteers, the approach facilitates the identification of patient-specific CMB-related connectomic changes while incorporating the ability to perform group analyses. This pipeline for the identification and profiling of connectopathies can assist the adaptation of clinical rehabilitation protocols to patients' individual needs.

ACM-BCB'18, August 29-September 1, 2018, Washington, DC, USA.

ACM ISBN 978-1-4503-5794-4/18/08...$15.00
https://doi.org/10.1145/3233547.3233598

CCS CONCEPTS

• Applied computing → Life and medical sciences; Computational biology; Biological networks, Imaging

KEYWORDS

Neuroinformatics; data science; brain connectome; magnetic resonance imaging

ACM Reference format:

A. Maher, K. Rostowsky, N. Chowdhury, and A. Irimia. 2018. Neuroinformatics and analysis of connectomic alterations due to cerebral microhemorrhages in geriatric mild neurotrauma. In *Proceedings of 9th ACM Conference on Bioinformatics, Computational Biology, and Health Informatics (ACM-BCB '18). ACM, New York, NY, USA, 8 pages.*

1 INTRODUCTION

The neuroinformatic analysis of structural magnetic resonance, diffusion-weighted and diffusion tensor imaging (sMRI, DWI and DTI, respectively) acquired from traumatic brain injury (TBI) patients can help neuroscientists to understand how brain network changes can lead to measurable neurological deficits [1]. Despite the potential of personalized neuroimaging analysis for neurotrauma patients, the range of algorithmic approaches for quantifying injury- related alterations to white matter (WM) networks remains limited and there are few informatics solutions for streamlining subject-level analyses [2]. Nevertheless, the ability to examine brain networks on a patient-by-patient basis when quantifying network degradation after lesion onset remains desirable not only in mild TBI (mTBI) but also in multiple sclerosis (MS), stroke, and brain cancer.

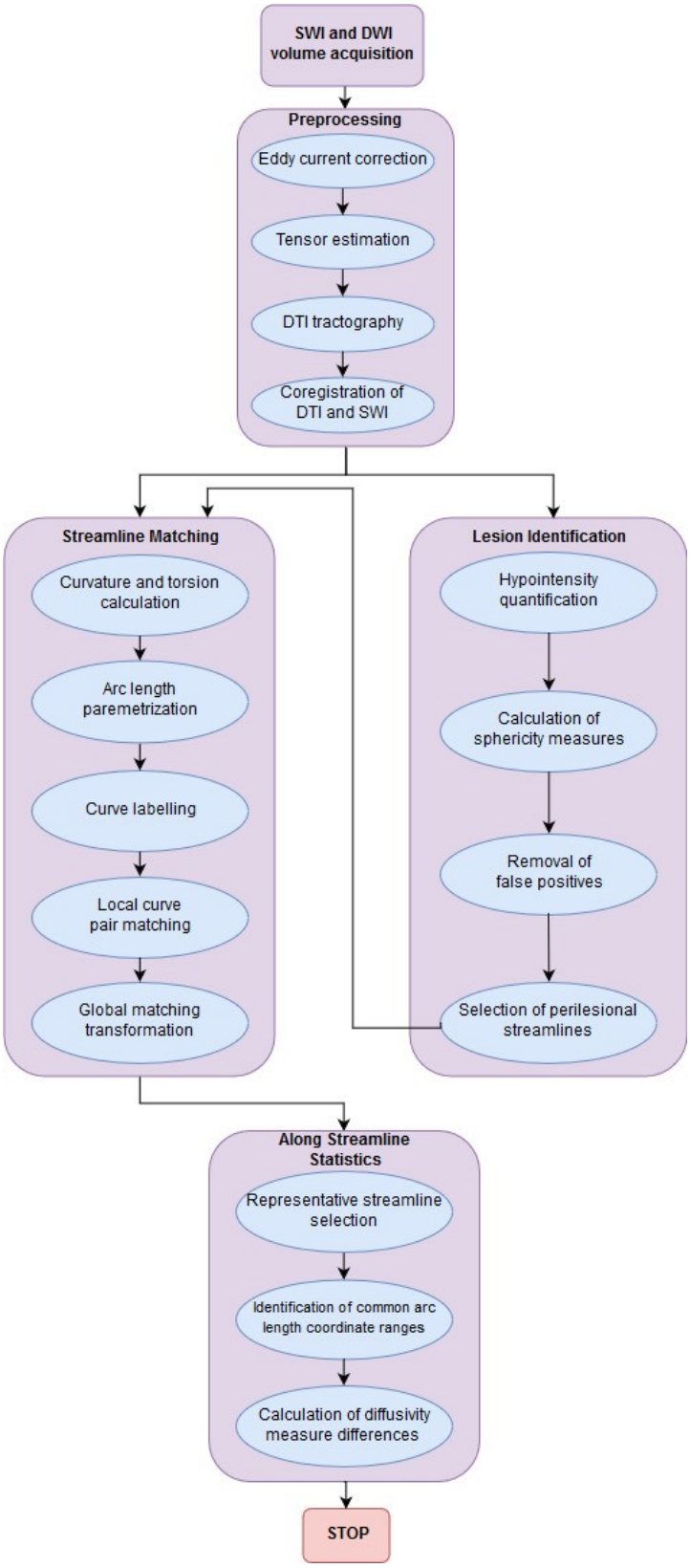

Fig. 1. Flowchart of neuroimage analysis for SWI/DWI volumes (see text for details).

Understanding how neural injuries can affect brain networks remains an important task due to the association between connectopathies and the degradation of neurocognitive function. By designing novel neuroinformatics workflows for the patient-tailored longitudinal analysis of brain networks, the refinement of rehabilitation protocols for these victims of neurovascular pathology can be facilitated.

This study demonstrates a novel approach to the patient-tailored assessment of injury-related longitudinal changes in the macroscale connectome. Our analysis of DWI/DTI measurements from healthy control (HC) older adults and from age- and sex-matched mTBI victims with MRI-detectable cerebral microbleeds (CMBs) demonstrates the ability to situate individual patients relative to a user-defined control population. Importantly, the approach preserves and enhances the neuroinformatician's ability to undertake group-level studies in this highly heterogeneous clinical population and our pipeline has potential applications ranging from the quantification of local connectivity changes in perilesional areas to the detection of global reorganization of brain networks.

2 MATERIALS AND METHODS

A flowchart which summarizes the data processing and analysis steps is shown in Fig. 1.

2.1 Participants and recruitment

This study was implemented in conformity with US federal law (45 C.F.R. 46) and was approved by the Institutional Review Board (IRB) at the University of Southern California (USC). All materials and methods follow the relevant directives and guidelines enforced by the USC IRB. mTBI-related CMBs are often observed in older brain trauma victims [1], and all participants in this study were aged 65 or older at the time of enrollment. Exclusion criteria included (1) a history of neurological or psychiatric disease and (2) the presence of structural neuropathology (aside from CMBs) on MRI scans. Two groups (26 mTBI patients and 26 HC volunteers) were included, with a 1:1 sex ratio in each group. The Glasgow Coma Scale (GCS) scores of mTBI patients were available (mean $\mu = 13.7$, standard deviation $\sigma = 0.4$). Welch's t test was implemented to determine whether there were significant differences in age or GCS score between mTBI patients and HC volunteers.

2.2 Neuroimaging

The same MRI scanner type (Prisma MAGNETOM Trio TIM, 20-channel head coil, 3 T magnetic field strength, Siemens Corp., Erlangen, Germany) was used to acquire gradient-echo (GE) DWI as well as anatomic MRI volumes [T_1- and T_2-weighted MRI, gradient-recalled echo (GRE)/susceptibility weighted imaging (SWI)]. To acquire T_1-weighted MRI, a three-dimensional (3D), magnetization-prepared rapid acquisition gradient echo (MPRAGE) sequence was used [repetition time (T_R) = 1,950 ms; echo time (T_E) = 2.98 ms; inversion time (T_I) = 900 ms; echo train length (ETL) = 1; flip angle = 9 degrees; field of view (FOV) = 256 mm × 256 mm; matrix size = 256 × 256; slice thickness = 1 mm]. T_2-weighted volumes were acquired using a 3D sequence (T_R = 2,500 ms; T_E = 360 ms; flip angle = 120 degrees; ETL = 180; FOV = 256 mm × 256 mm; matrix size = 256 × 256; slice thickness = 1 mm). Flow-compensated GRE/SWI volumes were acquired axially (T_R = 30 ms; T_E = 20 ms; FOV = 256 mm × 192 mm; matrix size = 512 × 256; slice thickness = 2 mm). DWI volumes were acquired axially in 64 gradient directions (T_R = 8,300 ms; T_E = 72 ms; flip angle = 90 degrees; FOV = 256 mm × 256 mm; acquisition matrix size = 128 × 128; slice thickness = 2 mm). Two DWI volumes with b = 0 s/mm^2 and b = 1,000 s/mm^2 (where b is the diffusion-weighting constant of DWI) were also procured. mTBI volunteers were imaged acutely (~2 days after injury) and chronically (~6 months post-injury). HC volunteers were scanned twice, within a six-month interval.

2.3 DTI streamline matching

To quantify within-subject neural network circuitry differences across time, an algorithm for matching DTI tractography streamlines across time points was integrated within the analysis pipeline. Based on the algorithm developed by Leemen et al, each streamline was modeled as a piecewise-differentiable 3D space curve with curvature κ and torsion τ, both of which are rotationally- and translationally-invariant topological properties of the curves corresponding to DTI tractography bundles [4]. By calculating κ and τ, corresponding space curves were labeled, local transformations of curve pairs were calculated, and a global transformation was computed [5]. Arc-length parametrizations, with point correspondences across time, were generated for each perilesional streamline bundle and within each subject. A curve index correspondence was established for every such space curve, across each time point and within each subject. A local transformation was computed to implement point-to-point co-registration utilizing Schönemann's solution to the orthogonal Procrustes problem [5]. By minimizing the global residues of squared inter-curve distances, a global transformation mapping source curves to target curves was then estimated from local curve transformations.

2.4 Lesion analysis

Lesions were identified both by a human expert with training in neuroradiology/neuropathology and by an automated algorithm which was integrated within the processing pipeline. The automated algorithm used a voxel classifier utilizing the Microbleed Anatomic Rating Scale [6] to label potential CMB image features. Identification was performed based on GRE/SWI scans, where hypointensities are indicative of CMB presence. Accounting for CMB shape by creating a separate pipeline module allowed lesions which had been erroneously identified as such (i.e. false positives) to be omitted.

A modified version of a streamline affinity approach originally proposed by O'Donnell & Westin [7] was used in conjunction with a method for distance mapping [8] to obtain streamline prototypes for curves matched across time points. The first of these algorithms requires choosing a streamline which best represents a bundle's spatial trajectory. In other words, for each streamline bundle, a curve portion which is appropriate for the calculation of along-streamline statistics must be identified because of variability in streamlines lengths. A range of arc-length coordinates common to each streamline within a bundle being analyzed is chosen along each curve portion. Subsequently, along-streamline measures of diffusivity—such as fractional anisotropy (FA)—is calculated for each streamline's arc-length coordinates along with descriptive statistics for every point [7]. For perilesional streamlines, between-scan differences in mean FA were identified. This DTI measure was used due to the prevalence of its use in DTI studies and because it is based on all three eigenvalues of the diffusion tensor, thereby reportedly conveying more information about streamlines than radial or axial diffusivity alone. Because the number of CMBs can vary substantially across mTBI patients, the workflow was designed to accommodate the parallel—rather than sequential—analysis of each CMB. This computationally efficient feature allows more uniform distribution of the computational load across processors and is also most useful when (A) the number of subjects and imaging volumes with CMBs is large and/or (B) there is substantial variability in the number of identified CMBs across subjects. These features of our pipeline are likely to be even more useful in future studies which focus on moderate and severe TBI, and where the number of CMBs can be very large.

3 RESULTS

3.1 Demographics and pathology findings

The average age difference between HC and mTBI volunteers was not found to be significant (Welch's $t_{23.93}$ =-0.78, $p > 0.77$); the mean GCS score difference between the TBI and HC groups was found to be statistically significant, as expected (Welch's t_{12} = -34.55, $p < 2.14 \times 10^{-17}$). By design, there was no sex ratio difference between samples. The automated algorithm for CMB identification was found to have a sensitivity of 94.4% (σ = 4.2%). No CMBs were identified in HC participants. In mTBI patients, CMB counts were found to range between 2 and 13 (μ = 6.04, σ = 2.63).

3.2 DTI-derived connectivity

In Fig. 2, the DTI-derived corpora callosa of two mTBI victims are superimposed on their respective MPRAGE T_1-weighted images. Each pair of differently colored streamlines depicts the corpus callosum at one of the two time points where MRI recordings were acquired. The reconstructions are of sufficient quality to enable the visualization of major streamline bundles within the corpus callosum and to inspect the homogeneity of their spatial overlap across time points. Comparison of Fig. 2 to reference neuroanatomical reconstruction of the corpus callosum reinforces the impression of its adequate reconstruction [9]. Although similar, the two pairs of reconstructions exhibit subtle differences which are emphasized by the fact that different colors are used to depict them.

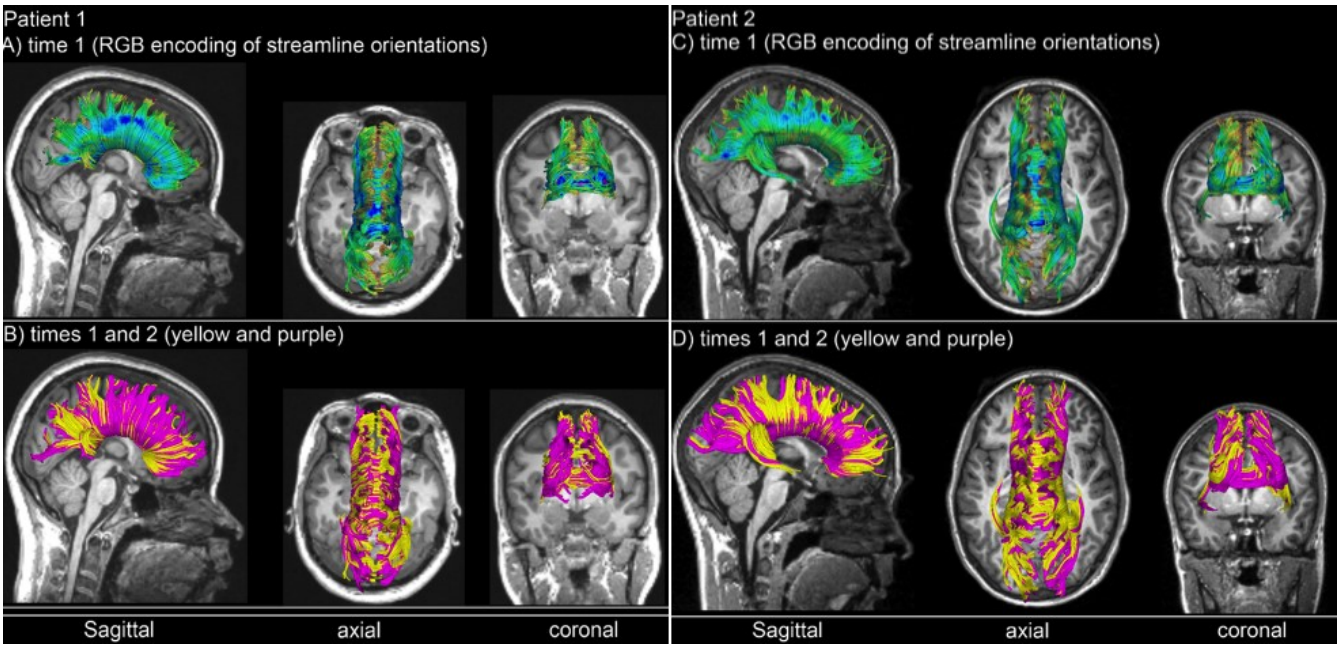

Fig. 2. DTI-constrained reconstructions of the corpus callosum in two representative mTBI patients (Patient 1: A and B; Patient 2: C and D). Insets A and C depict RGB-encoded streamline orientations for the acute scan of each patient. Insets (B) and (D) help to visualize differences in WM streamline locations across time points. These may be due to pathology-related processes, to DWI/DTI artefacts or to other confounds.

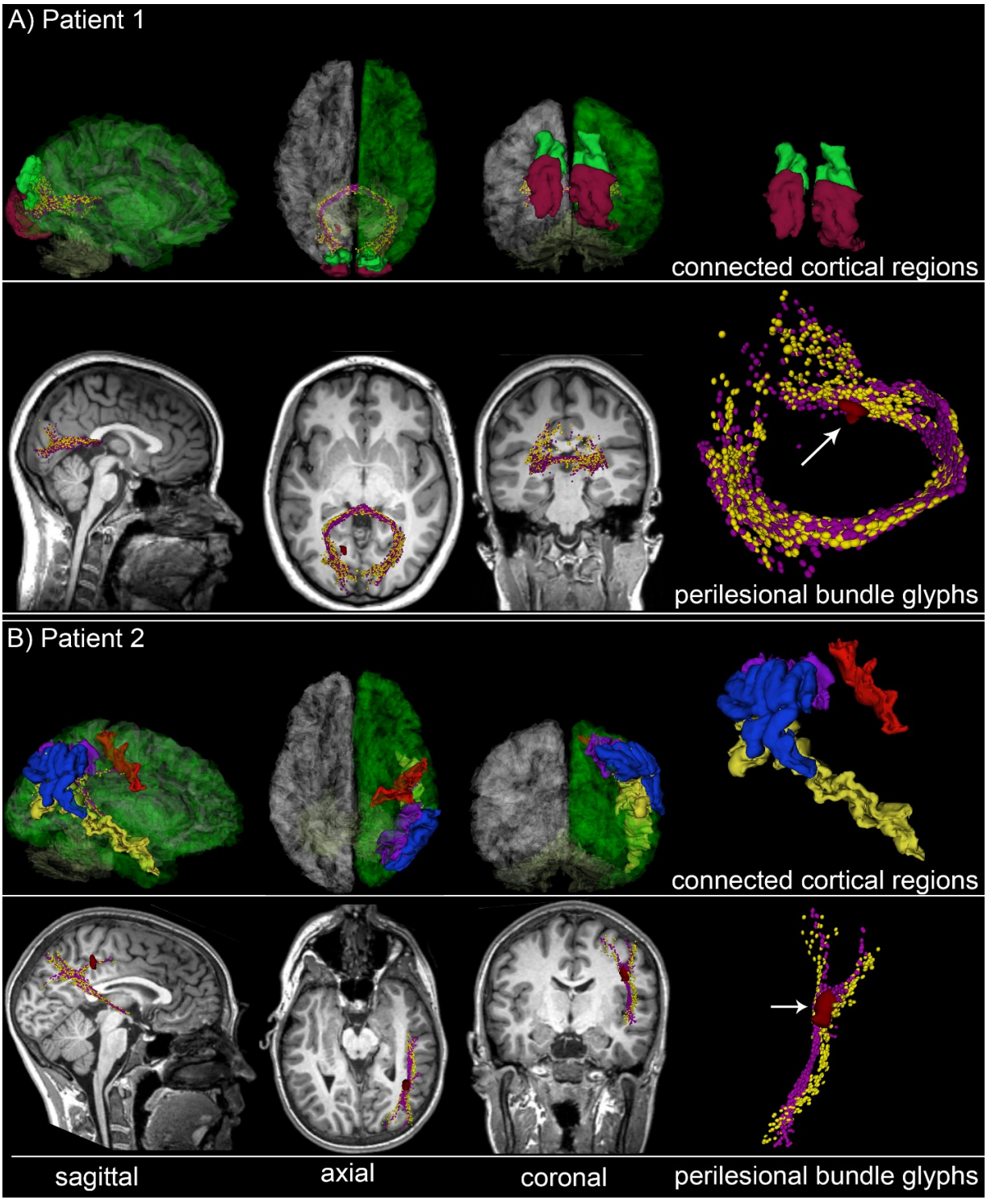

Fig. 3. Reconstructions of DTI streamline bundles (acute: yellow; chronic: magenta) which are adjacent to CMBs identified in two mTBI victims (Patient 1: A and B; Patient 2: C and D). Cortical models (translucent green) are overlaid onto T1-weighted images to assist with the visualization of CMB locations relative to brain landmarks and to the trajectories of perilesional streamlines. Cortical regions innervated by perilesional streamline bundles are shown as well, both in relation to the entire cortex (sagittal, axial, coronal views, left three columns) and separately (rightmost column).

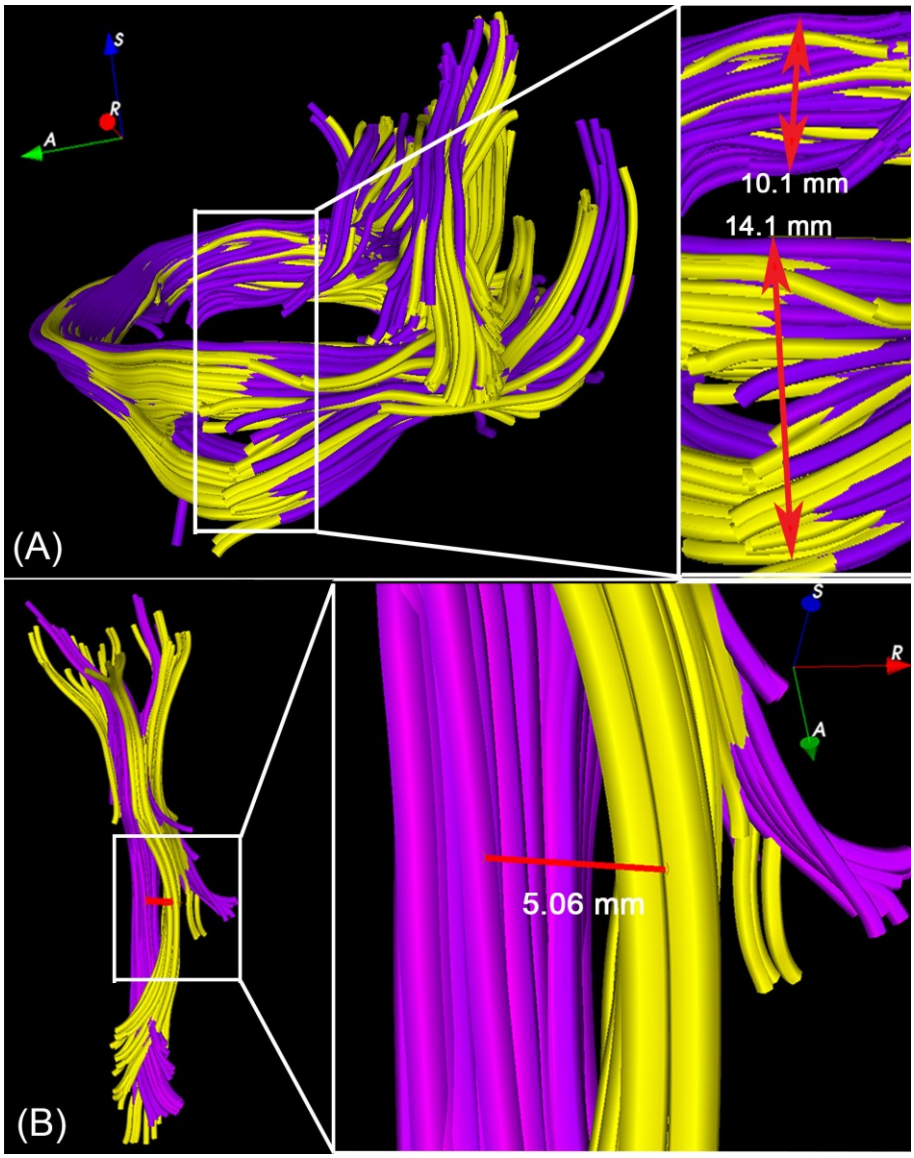

Fig. 4. Fiducial measurements of WM streamline displacements in Patients 1 (A) and 2 (B). WM bundles are displayed for both the acute (yellow) and chronic (magenta) time points. Insets are used to show regions of interest in more detail. Red lines are drawn between fiducial points at locations of maximal displacement. For convenience, coordinate system axes (R = right, A = anterior, S = superior) are shown for both patients. (A) The portion of the callosal splenium ipsilateral to the CMB is found to be 4 mm thicker than the contralateral portion. (B) The displacement experienced by the largest WM streamline is found to be greater than 5 mm.

These differences may be a result of network alterations due to injury, though they may be caused partially by tractography inaccuracies, motion and by other confounds, as discussed in what follows.

3.3 DTI streamline matching

Fig. 3A displays the MRI scans of two mTBI victims exhibiting CMBs in the WM. The streamline bundles associated with each patient's corresponding CMB are shown using glyphs. Patient 1 is a male mTBI victim whose splenial callosal fibers are near a ~4 mm^3 CMB in the left-hemisphere. Upon inspection of perilesional streamlines, one can note an asymmetry in streamline trajectories with respect to the longitudinal fissure. Specifically, the trajectories of streamlines ipsilateral to the CMB diverge visibly in the perilesional neighborhood; this abnormality is observed in both acute and in chronic scans, suggesting that CMBs may conceivably alter WM architecture in their neighborhood. Patient 2 (Fig. 3B) is a male mTBI victim (GCS = 13) with a ~3 mm^3 CMB. This patient made an upper-good recovery (GOS-E = 8); his CMB is near a streamline bundle which links the right temporal lobe to the right parietal lobe. Upon comparison of acute and chronic time points, a post-injury

shift of the longest streamline bundle toward the right lateral ventricle is apparent (Fig. 4). These results support the possibility that CMBs may be associated with alterations in neural network circuitry, despite modest CMB sizes. Future research should study these effects in larger samples.

4 DISCUSSION

Many methods for neural network analysis which have received attention from neuroinformaticians—e.g. voxel-based morphometry (VBM), tract-based spatial statistics (TBSS), and automated longitudinal intra-subject analysis (ALISA)—implement subject averaging to create fiber skeletons and/or atlases for group analysis. This study proposes a patient-specific approach which allows one to identify tract correspondences from longitudinal scan series in the presence of CMBs. VBM uses location-specific statistical tests of FA differences to reduce image misalignment by projecting an approximate nonlinear registration onto an alignment-invariant tract known as the FA skeleton. Although TBSS was introduced to address some disadvantages of VBM [10], the method proposed here has at least one considerable advantage over TBSS in that it can be used for longitudinal neural network analysis at arbitrary locations in the WM, i.e. both near and far from the traditional TBSS skeleton. Another method—proposed by Yushkevich et al. [11] to address the shortcomings of TBSS—focuses on specific neural network modules of interest and may thus be of broader application. This approach, however, does not account for neuroanatomical changes due to neurodegeneration or to pathological conditions, whereas our method does. In our data analysis workflow, tractography is performed at each time point within a given subject and the resulting streamlines are matched across time points. One alternative is to co-register DWI volumes and only then to perform tractography; this approach, however, results in streamlines whose similarity is artificially driven by the volume co-registration process rather than by actual differences in neural network structure. In the method proposed here, individual structures are first generated and only then matched across time points to ensure realistic comparisons of streamline trajectories.

A successful approach to curve index correspondence is the streamline prototyping method [12; 13], where a prototype streamline is identified for an entire bundle. In our case, this method is useful because DWI measurements in perilesional areas may be confounded by motion or artefact, such that relying solely on tractography results without streamline prototyping can lead to substantial errors. These errors can often occur because perilesional streamlines may belong to more than one major bundle and because they can have paths of varying uniformity. In such cases, utilizing streamline prototypes along WM bundle trajectories can help to reduce the effects of confounds such as motion, structural changes, noise and other factors which might impair analysis.

The O'Donnell-Westin streamline affinity approach is suitable for our desired application due to its stability [7]. This method utilizes a process which is conceptually similar to the application of a low-pass, three-dimensional spatial filter to DWI/DTI image intensities to identify the most significant and topologically-consistent directions of water diffusion within a region of interest. By accounting for neural network topology and for individual neuroanatomy, the result is a more principled way of mitigating the effects of motion artifacts, measurement noise, and of other confounds.

5 CONCLUSIONS

Neuroinformatics approaches to the visualization and quantification of connectomics changes can be used to identify so-called connectopathies as well as potential relationships between neural network changes and neural/cognitive deficits on a patient-by-patient basis. The primary clinical appeal of the longitudinal analysis method proposed in this study involves the mapping and analysis of changes in neural networks after the onset of mTBI-related CMBs. When combined with fMRI and/or electrophysiological measurements, approaches like ours can provide insight into neuropathology evolution and may help to clarify the relationship between changes in neural network topology and the associated neurocognitive deficits of brain injury patients.

ACKNOWLEDGMENTS

The authors declare no actual or perceived conflict of interest. This research was supported by the National Institute of Neurological Disorders and Stroke, grant R01 NS100973.

REFERENCES

[1] S.M. Greenberg, M.W. Vernooij, C. Cordonnier, A. Viswanathan, R.A.S. Salman, S. Warach, L.J. Launer, M.A. Van Buchem, M.M.B. Breteler, and Microbleed Study Group, Cerebral microbleeds: a guide to detection and interpretation. Lancet Neurol vol. 8, pp. 165-174, 2009.

[2] P. Mukherjee, S.W. Chung, J.I. Berman, C.P. Hess, and R.G. Henry, Diffusion tensor MR imaging and fiber tractography: Technical considerations. Am J Neuroradiol vol. 29, pp. 843-852, 2008.

[3] J.G. Sled, A.P. Zijdenbos, and A.C. Evans, A nonparametric method for automatic correction of intensity nonuniformity in MRI data. IEEE Trans Med Imaging vol. 17, pp. 87-97, 1998.

[4] A. Leemans, J. Sijbers, S. De Backer, E. Vandervliet, and P. Parizel. Multiscale white matter fiber tract coregistration: A new feature-based approach to align diffusion tensor data. Magn Reson Med vol. 55, pp. 1414-1423, 2006.

[5] A. Leemans, and D.K. Jones, The B-matrix must be rotated when correcting for subject motion in DTI data. Magn Reson Med vol. 61, pp. 1336-1349, 2009.

[6] S.M. Gregoire, U.J. Chaudhary, M.M. Brown, T.A. Yousry, C. Kallis, H.R. Jager, and D.J. Werring, The Microbleed Anatomical Rating Scale (MARS) reliability of a tool to map brain microbleeds. Neurology vol. 73, pp. 989-994, 2006.

[7] L.J. O'Donnell, and C.F. Westin, Automatic tractography segmentation using a high-dimensional white matter atlas. IEEE T Med Imaging vol. 26, pp. 1562-1575, 2007.

[8] M. Maddah, W.E.L. Grimson, S.K. Warfield, and W.M. Wells, A unified framework for clustering and quantitative analysis of white matter fiber tracts. Med Image Anal vol. 12, pp. 191-202, 2008.

[9] S. Hofer, and J. Frahm, Topography of the human corpus callosum revisited - Comprehensive fiber tractography using diffusion tensor magnetic resonance imaging. Neuroimage vol. 32, pp. 989-994, 2006.

[10] S.M. Smith, H. Johansen-Berg, M. Jenkinson, D. Rueckert, T.E. Nichols, K.L. Miller, M.D. Robson, D.K. Jones, J.C. Klein, A.J. Bartsch, and T.E.J. Behrens, Acquisition and voxelwise analysis of multi-subject diffusion data with Tract-Based Spatial Statistics. Nat Protoc vol. 2, pp. 499-503, 2007.

[11] P.A. Yushkevich, H. Zhang, T.J. Simon, and J.C. Gee, Structure-specific statistical mapping of white matter tracts. Neuroimage vol. 41, pp. 448-461, 2008.

[12] M. Maddah, W.E.L. Grimson, and S.K. Warfield, Statistical modeling and EM clustering of white matter fiber tracts. I S Biomed Imaging pp. 53-56, 2006.

[13] P.G. Batchelor, F. Calamante, J.D. Tournier, D. Atkinson, D.L.G. Hill, and A. Connelly, Quantification of the shape of fiber tracts. Magn Reson Med vol. 55, pp. 894-903, 2006.